Cite this: DOI: 10.1039/c6mh00419a

Chemical tuning of Coulomb blockade at room-temperature in ultra-small platinum nanoparticle self-assemblies†

DOI: 10.1039/c6mh00419a

Simon Tricard, *[a] Olivier Said-Aizpuru, [a] Donia Bouzouita,[a] Suhail Usmani,[a] Angélique Gillet,[a] Marine Tassé,[b] Romuald Poteau, [a] Guillaume Viau,[a] Phillipe Demont,[c] Julian Carrey[a] and Bruno Chaudret[a]

This work describes self-assemblies of ultra-small platinum nanoparticles, the electrical properties of which can be adjusted through slight modifications of the assemblies' constituents. Elaborating such systems, stable in air for months, is a first step towards nanoelectronic systems, where the charging energy of the nanoparticles is tuned by the nature of the ligands.

If the use of metallic nanoparticles (NPs) in molecular electronic devices is to be developed, a first prerequisite will be to control Coulomb blockade (CB) – *i.e.* the gap at low voltage in which no current flows.[1–3] However, although one and two-dimensional systems are already described,[4–6] three main features are still lacking toward this goal in three dimensional metallic NP assemblies: (1) chemical tools that subtly control the strength of CB,[7,8] (2) systems sufficiently robust to remain stable for months in air at room temperature, and (3) versatile electric properties, measurable at all scales, to facilitate potential integration into devices. Molecule/NP self-assemblies (SAs) are appropriate systems to do so, as both molecules and NPs can be finely adapted to tune the three experimental parameters important for controlling the NP charging energy: (1) the size of the NPs, (2) the distance between them and (3) the dielectric constant of the ligands.[9,10] CB has previously been described in metallic NP SAs, and some ligand effect has been well documented for measurements at low temperatures.[4,5,11–15] To observe CB at room temperature with metallic objects, it is important to work with ultra-small objects (<2 nm in size), as shown for Au_{55} nanoclusters,[16] Au NPs,[17,18] or Au, Pt, Pd or Co clusters obtained by physical processes: sputtering,[19–22] evaporation,[23–25] or pulsed laser deposition.[26] In this work, we chose air-stable ultra-small (1.1 to 1.7 nm) platinum NPs – in the same size range as the considered molecules – connected by simple alkyl or aryl thiol ligands, which form strong Pt–S bounds with the NP surface. The sizes of the ligands are modified to tune the inter-particle distance and their functional groups to tune their dielectric constant. We obtained robust systems, stable in air for months, displaying CB at room temperature, which depends on the nature of the ligand. We also succeeded in addressing the SAs at different scales: nano (~10 nm), micro (~1 μm), and macro (~0.1 mm). The originality of our approach is the use of direct synthesis of ultra-small NPs from organometallic precursors, which gives high potentiality to finely control the average size of the NPs, and the nature and the quantity of ligands at the surface of the NPs.

Platinum NPs were prepared by decomposition of $Pt_2(dba)_3$ (dba = dibenzylideneacetone) under a carbon monoxide (CO) atmosphere in THF,[27] followed by complete elimination of the organic ligands by washing with pentane, as confirmed by Fourier-transform infrared (FT-IR) spectroscopy (Fig. S1, ESI†). These "naked" NPs were only stabilized by CO and the coordinating solvent, THF. Their average size is 1.1 nm after the synthesis and can increase up to 1.7 nm upon ripening in solution.

Conceptual insights

Even though Coulomb blockade has been studied for over sixty years, and previously observed at room temperature, the new concept here is its fine modulation, which can only be achieved by a controlled organometallic chemistry approach, as a first step toward electronic devices. The goal is to tune Coulomb blockade in dense three-dimensional self-assemblies of metallic nanoparticles with simple chemical tools. Synthesizing robust systems – stable in air for months – is a crucial condition; platinum nanoparticles stabilized by thiols, which form strong Pt–S bonds, are thus suitable systems. This article describes the first system where the nanoparticle size, the ligand length and the ligand dielectric constant are independently varied to control the nanoparticle charging energy. Such a chemical approach allowed the determination of the most important parameters that influence Coulomb blockade, namely the dielectric constant of the ligands and the size of the nanoparticles.

[a] *LPCNO, INSA, CNRS, Université de Toulouse, 31077 Toulouse, France. E-mail: tricard@insa-toulouse*

[b] *LCC, CNRS, Université de Toulouse, 31077 Toulouse, France*

[c] *Institut Carnot – CIRIMAT, Université de Toulouse, 31062 Toulouse, France*

† Electronic supplementary information (ESI) available: Experimental methods, references for DFT calculations, discussion on axial *vs.* global polarizability, supplementary characterization, and experimental values. See DOI: 10.1039/c6mh00419a

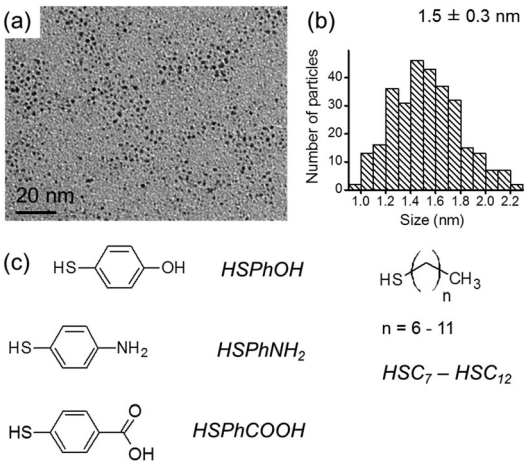

Fig. 1 (a) TEM micrograph and (b) size distribution of the naked platinum nanoparticles. (c) Chemical structures of thiol ligands: one aryl series varying the terminal functional group (left), and one alkyl series varying the length of the molecule (right). Abbreviated names are given in italics.

For each size, transmission electronic microscopy (TEM) images show well dispersed objects with a size dispersion of ~20 to 30% (Fig. 1a and b). The addition of thiol ligands stops the ripening process. This procedure offers the possibility to precisely tune the concentration and the nature of the surface ligands. Two series of thiols were investigated: an aryl one, with three functional groups that can interact by hydrogen bonding (4-mercaptophenol HSPhOH, 4-aminothiophenol $HSPhNH_2$ and 4-mercaptobenzoic acid HSPhCOOH), and an alkyl one, with linear chains that can interact with each other by van der Waals interactions, with an increasing number of carbons from seven (heptanethiol HSC_7) to twelve (dodecanethiol HSC_{12}) (Fig. 1c). The equivalent number (eq.) is defined as the ratio between the quantity of ligands and the quantity of platinum atoms present in the system.

Four SAs were studied with naked NPs displaying an intermediate size of 1.5 nm and 0.1 to 0.4 eq. of HSPhOH. In all the conditions, microscopic rod-shaped SAs were formed, without any significant morphologic differences, as evidenced by TEM imaging (Fig. 2a–d). The global shape and the size distribution of the individual NPs remained unchanged after the coordination of the ligand and the assembly process, as demonstrated both by TEM (Fig. 2e and f) and X-ray diffraction (XRD) measurements (Fig. S2, ESI† – the platinum particles are single crystals adopting the fcc structure). For 0.1 eq. and 0.2 eq., the IR spectra of the NPs evidenced a red-shift of the aromatic CC bonds' wavenumbers between 1460 and 1620 cm^{-1} (Fig. 2g and Fig. S3, ESI†). This behavior reflects a weakening of the chemical bonds, attributed to the participation of the aryl rings in SA formation. For 0.3 eq. and higher, a shoulder is visible at the position of the free ligand, indicating an excess of molecules. We thus chose to further investigate the systems at 0.2 eq., to avoid any excess of free ligands.

To prove the fine tuning of our SAs, we first investigated the control of the inter-particle distances. We thus synthesized SAs with 1.3 nm naked NPs and alkyl thiols, increasing the number of carbons one by one from HSC_7 to HSC_{12}. Here too the

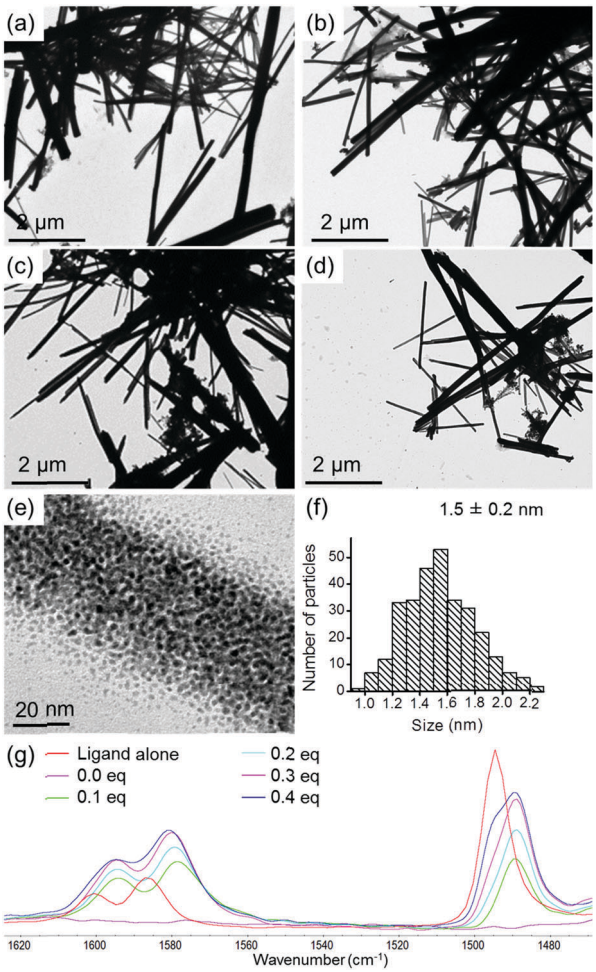

Fig. 2 TEM micrographs of the self-assemblies after addition of HSPhOH: (a) 0.1 eq., (b) 0.2 eq., (c) 0.3 eq., and (d) 0.4 eq. (e) TEM micrograph at higher magnification and (f) size distribution of the platinum nanoparticles in the self-assemblies with 0.2 eq. of ligand. (g) FT-IR spectra of the aromatic CC vibrations of the ligand alone and of the ligands within the self-assemblies (from 0.0 to 0.4 eq.). The spectra are normalized to the signal of the CO vibration at 2040 cm^{-1}, as seen in Fig. S3, ESI.†

SAs consisted of micrometric rods made of nanometric NPs (Fig. 3a and b). The inter-particle distances were determined by small angle X-ray scattering (SAXS). For the six samples, correlation peaks were observed on SAXS patterns, with the position of the maximum intensity progressively shifting towards lower q values when the length of the molecule increased (Fig. 3c). We observed that the corresponding correlation distance s, estimated according to $s = 2\pi/q_{max}$,[28] linearly increased as a function of the carbon number with a slope of 123 ± 8 pm per C (Fig. 3d). A structural model shows that the projection of a C–C bond on the axis of an alkyl chain in all-*trans* conformation is equal to 125 pm (Fig. 3e). These geometric considerations are thus in very good agreement with a precise tuning of the inter-particle distance s at the scale of a carbon–carbon length.

Similarly, large SAs were formed upon using small 1.2 nm NPs and a series of three aryl thiols, where the functional group in the *para* position changed. Platelets were formed when using $HSPhNH_2$, rods using HSPhOH, and larger rods using

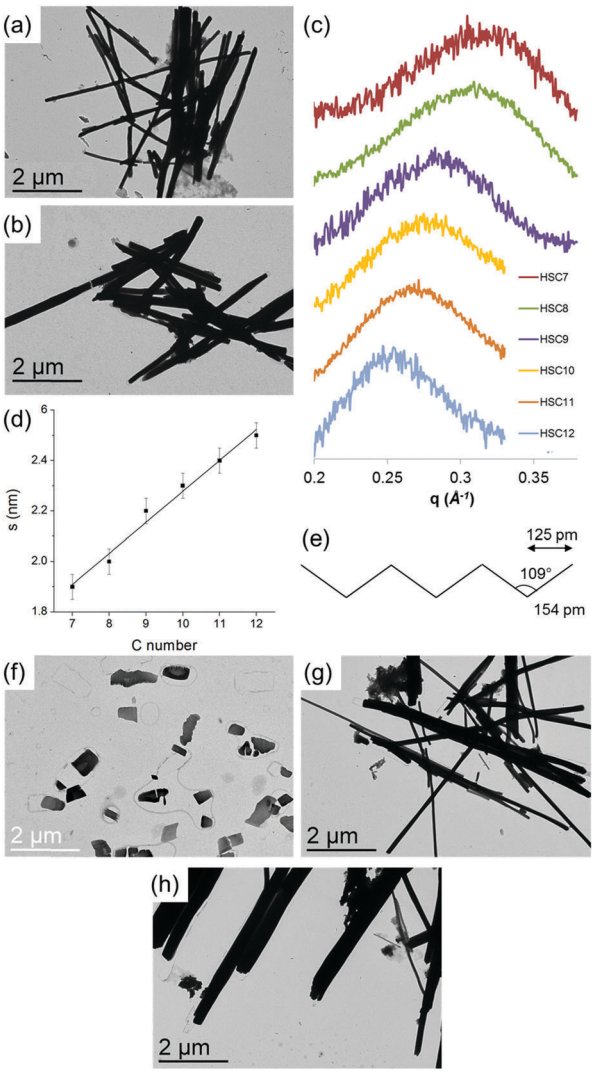

Fig. 3 TEM micrographs of the self-assemblies after addition of 0.2 eq. of alkyl ligands: (a) HSC_8, (b) HSC_{12}. (c) Small angle X-ray scattering patterns for the six ligands (HSC_7 to HSC_{12}). (d) Evolution of the correlation distance s as a function of the number of carbons, and linear regression (slope: 123 ± 8 pm per C). (e) Geometrical model of an alkyl chain and characteristic bond lengths. TEM micrographs of the self-assemblies after addition of 0.2 eq. of: (f) $HSPhNH_2$, (g) HSPhOH, and (h) HSPhCOOH.

HSPhCOOH (Fig. 3f–h). Interestingly, larger dimension SAs were formed when the strength of hydrogen bonds between functional groups increased (amine < hydroxyl < carboxylic acid). 1.7 nm-large NPs gave similar SAs, both in shape and size of superstructures. SAXS measurements gave s distances between 1.6 and 2.1 nm, with larger s for larger NPs (Fig. S4 and Table S1, ESI†).

Such arrays of ultra-small NPs offer the possibility to measure charge transport. The mechanism of such a charge transport is still debated in the literature.[5,29–33] However, it is commonly admitted that the electron mobility is limited by the charging energy of a NP, defined as $E_C \sim e^2/(2\pi\varepsilon_r\varepsilon_0 d \ln(s/(s-d)))$, where e is the charge of the electron, ε_0 the permittivity of vacuum, ε_r the dielectric constant of the medium surrounding the particles, d the particle diameter, and s the center-to-center distance between two particles.[10,34] Three parameters can be experimentally tuned: s, d and ε_r. The alkyl series allowed a precise variation of s, keeping d constant as we used the same starting particles. The aryl series investigated the influence of variation of d, as two NP sizes were chosen (d = 1.2 and 1.7 nm). In addition, the substitution of the moiety in the *para* position to the thiol aryl groups significantly affected ε_r. The dielectric constants of the free ligands were measured by dielectric spectroscopy on powders of free ligands: ε_r = 7.1 for $HSPhNH_2$, 5.2 for HSPhOH, and 2.7 for HSPhCOOH.

In order to measure their electronic characteristics, the HSC_7 alkyl chain stabilized SAs were deposited by dielectrophoresis on an interdigitated combs device, with spacing between the electrodes equal to 5 μm (Fig. 4a-micro).[9,10] *I–V* curves measured at temperatures ranging from 100 to 300 K (Fig. 4b) reveal the presence of CB, with a power law characteristic that depends on temperature.[31] We thus confirm that precise control of the NP size below 2 nm leads to assemblies displaying CB at room temperature. However, quantitative comparison between SAs containing different ligands was impossible using the interdigitated comb method, because of a large variability in the NP density from comb to comb. To circumvent this drawback, we elaborated a new approach combining charge transport measurements by conductive atomic force microscopy (CAFM) and statistical analyses. The rods were drop-cast on a gold surface and a large number of *I–V* curves (~50) were measured by contacting the CAFM tip on different individual SAs (Fig. 4a-nano). As the amplitude of the current strongly varied from SA to SA, the fifty curves were normalized at 5 V and averaged to compare the current characteristics of one sample to another one (Fig. 4c). CAFM measurements confirmed that the non-linear behavior in *I–V* curves was present at the nanoscale for all alkyl chain lengths, but also for all aryl thiols (Fig. 4d). Besides, CB was also present at the macroscopic scale in a large amount of materials (several milligrams – with HSPhOH), as observed by dielectric spectroscopy on a powder pressed between two 10 mm-wide electrodes, at temperatures ranging from 100 to 296 K (Fig. 4a-macro and Fig. 4e). We thus measured CB signatures at the nano-, micro- and macro-scales for all the SAs, at room temperature. Furthermore, the charge transport characteristics measured by CAFM remained constant for at least six months, for the three aryl ligands (Fig. S5, ESI†). Our SAs are thus extremely robust systems, which can stay stable for a long time in air at room temperature.

CB is related to the impossibility of charging single NPs at low bias. In the present case, it can be observed at room temperature thanks to the very small size of our NPs (down to 1.2 nm). The importance of the size of the particles d can be demonstrated in this system since differences in d as small as 0.5 nm are significant, as evidenced in Fig. 4d. For example, for the HSPhCOOH SAs, the current at a given voltage – directly linked to the strength of CB – is significantly smaller for the smaller NPs (*e.g.* at 0.7 V, $I/I(2V)$ = 0.04 for d = 1.2 nm and $I/I(2V)$ = 0.08 for d = 1.7 nm). Similarly, the influence of the dielectric constant surrounding the NPs ε_r is clear, as for example for the 1.2 nm NPs, where the current at a given voltage is smaller for ligands of lower

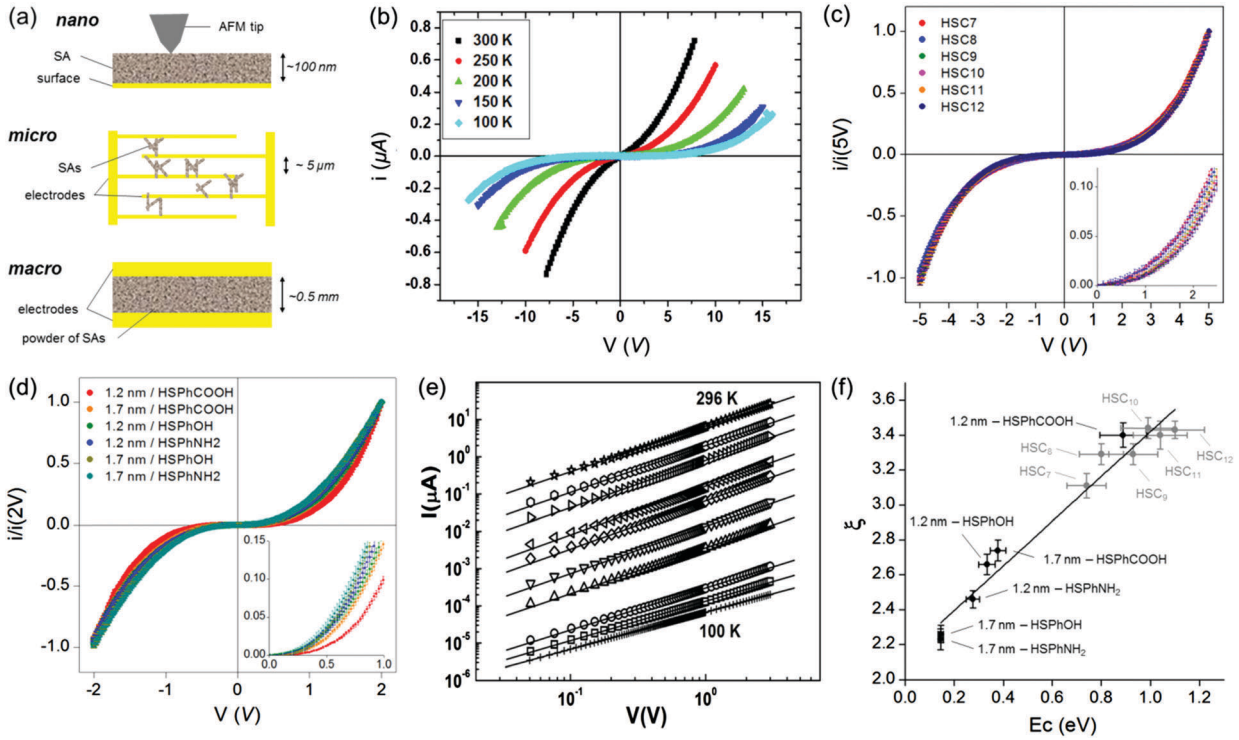

Fig. 4 (a) Schematics describing the charge transport measurements on self-assemblies (SAs) at three scales, and measurements: (b) at the microscale, performed with interdigitated combs with HSC_7, at temperatures ranging from 100 K to 300 K, (c) at the nanoscale, performed by conductive AFM measurements with the six alkyl ligands (HSC_7 to HSC_{12}), at room temperature; measurements are performed between −5 V and 5 V, the curves are normalized at 5 V; inset: magnification on the 0–2.5 V region, (d) at the nanoscale, performed by conductive AFM with $HSPhNH_2$, HSPhOH, and HSPhCOOH, and nanoparticles of 1.2 and 1.7 nm, at room temperature; measurements are performed between −2 V and 2 V, the curves are normalized at 2 V; inset: magnification on the 0–1 V region, (e) at the macroscale, performed by dielectric spectroscopy on a powder of self-assemblies with HSPhOH, at temperatures ranging from 100 to 296 K. (f) Evolution of the power exponent ξ (fitted from the *I*–*V* characteristics with aryl ligands – in black – and with alkyl ligands – in grey) as a function of the corresponding charging energies.

ε_r (*e.g.* at 0.7 V, $I/I(2V) = 0.04$ for HSPhCOOH – $\varepsilon_r = 2.7$ – and $I/I(2V) = 0.14$ for $HSPhNH_2$ – $\varepsilon_r = 7.1$). Finally, charge transport in SAs is also expected to depend on the inter-particle distance *s*, as previously reported.[10,17,24,28,32,35] However, when we focus on tiny distance variations, as precise as one single C–C bond, differences in CB are not evident to detect (Fig. 4c). For the alkyl series, the relatively small increase of CB as a function of *s* could be explained by a parallel increase of the ligand axial polarizability (calculated by DTF,[36] see below), which has an opposite effect to the inter-particle distance effect. This observation thus confirms a structuration of the alkyl thiols in a *trans* conformation in the SAs, as already suggested by the SAXS measurements.

Charge transport in SAs of metallic NPs have been studied in many groups and the transport mechanism is generally described as inelastic co-tunneling, resonant tunneling, variable range hopping, or nearest hopping.[7,9,11,13,14,25,28,33,34,36–40] However, most of these models have been validated at low temperatures, and they are system dependent, and generally refer to an ideal description of the assembly. But the size distribution of our NPs is not null. As the Coulomb energy is reciprocal to the diameter, the current will indeed flow preferentially through the largest particles (which are still small), but as thermal agitation is important at room temperature, pathways including smaller particles will also be activated. Size distribution is crucial to study physical mechanisms of charge transport, but it is not an issue here – at least *a posteriori*, as statistically significant effects are observed in charge transport for subtle modifications of the materials at the nanoscale. The physical model of charge transport is still under investigation in our specific systems, but current characteristics through the NP SAs can phenomenologically be described by the equation $I \propto V^{\xi}$, where the power exponent ξ is generally found between 2 and 3.5 in three-dimensional systems.[40] No significant threshold voltage has been observed; this parameter is not a good descriptive parameter for our measurements, in agreement with previous reports in the literature;[14] that is why we focused on the study of ξ (for details, see Justification of the fitting choice in the ESI†). Fig. 4f represents the evolution of ξ as a function of E_C. ξ is deduced from the experimental *I*–*V* curves and E_C has been calculated using $E_C \sim e^2/(2\pi\varepsilon_r\varepsilon_0 d \ln(s/(s-d)))$. A noticeably good correlation was observed between the evolution of the fitted ξ and the calculated charging energies (for details, see Discussion on axial *vs.* global polarizability, Tables S1–S3 and Fig. S6 in the ESI†). This result confirms that the evolution of CB can phenomenologically be described by the charging energy E_C, which depends only on *s*, *d* and ε_r. For some SAs, we obtained significantly high values of ξ – higher than 3, as generally reported. Such high values come from high Coulomb energies, but they can

also suggest charge transport mechanisms in three dimensions where electrons are highly constrained in percolation paths.[38,41]

In summary, we report here a study of the parameters governing CB at room temperature on a mixed molecule/NP self-assembled system. This system is characterized by the precise control of the NP size (1.2, 1.5 and 1.7 nm) as well as by the control of the ligand concentration on their surface thanks to the production of "naked" NPs, in fact stabilized only by CO and the solvent THF, and on which the desired quantity of ligands can be added. The versatility of this system allows, independently, the control of the three identified parameters governing CB in three dimensional assemblies, namely the size of the particles, the inter-particle distance and the dielectric constant of the ligand medium. By tuning these three factors, we were able to show that the main contributions come from the particle size and the dielectric constant surrounding the particles. The NP SAs proved to be air-stable for months and their electronic characteristics could be measured at the nanometric scale by CAFM, at the micrometric scale on interdigitated electrodes and at the macroscopic scale by dielectric spectroscopy, leading to convergent results. This system is therefore unique to control reproducibly CB in metallic NPs at room temperature and thus to develop novel molecule/NP electronics.

Acknowledgements

We thank Thomas Blon for gold evaporation on substrates. Financial support from the Agence Nationale de la Recherche (MOCANANO grant ANR-11-INTB-1011), the European Commission (BINOS grant PCIG11-GA-2012-317692), the Programme Investissements d'Avenir under the program ANR-11-IDEX-0002-02, reference ANR-10-LABX-0037-NEXT and the Indo-French Centre for the Promotion of Advanced Research – CEFIPRA is acknowledged.

Notes and references

1 W. Lu and C. M. Lieber, *Nat. Mater.*, 2007, **6**, 841–850.
2 C. Joachim, J. K. Gimzewski and A. Aviram, *Nature*, 2000, **408**, 541–548.
3 J. Liao, S. Blok, S. J. van der Molen, S. Diefenbach, A. W. Holleitner, C. Schönenberger, A. Vladyka and M. Calame, *Chem. Soc. Rev.*, 2015, **44**, 999–1014.
4 R. Parthasarathy, X.-M. Lin and H. M. Jaeger, *Phys. Rev. Lett.*, 2001, **87**, 18.
5 R. Parthasarathy, X.-M. Lin, K. Elteto, T. F. Rosenbaum and H. M. Jaeger, *Phys. Rev. Lett.*, 2004, **92**, 7.
6 V. Maheshwari, J. Kane and R. F. Saraf, *Adv. Mater.*, 2008, **20**, 284–287.
7 J. Liao, J. S. Agustsson, S. Wu, C. Schönenberger, M. Calame, Y. Leroux, M. Mayor, O. Jeannin, Y.-F. Ran, S.-X. Liu and S. Decurtins, *Nano Lett.*, 2010, **10**, 759–764.
8 D. V. Talapin, J.-S. Lee, M. V. Kovalenko and E. V. Shevchenko, *Chem. Rev.*, 2010, **110**, 389–458.
9 J. Dugay, R. P. Tan, A. Meffre, T. Blon, L.-M. Lacroix, J. Carrey, P. F. Fazzini, S. Lachaize, B. Chaudret and M. Respaud, *Nano Lett.*, 2011, **11**, 5128–5134.
10 J. Dugay, R. P. Tan, M. Ibrahim, C. Garcia, J. Carrey, L.-M. Lacroix, P.-F. Fazzini, G. Viau and M. Respaud, *Phys. Rev. B: Condens. Matter Mater. Phys.*, 2014, **89**, 041406.
11 R. P. Andres, T. Bein, M. Dorogi, S. Feng, J. I. Henderson, C. P. Kubiak, W. Mahoney, R. G. Osifchin and R. Reifenberger, *Science*, 1996, **272**, 1323–1325.
12 J. Liao, M. A. Mangold, S. Grunder, M. Mayor, C. Schönenberger and M. Calame, *New J. Phys.*, 2008, **10**, 065019.
13 A. Zabet-Khosousi and A.-A. Dhirani, *Chem. Rev.*, 2008, **108**, 4072–4124.
14 H. Moreira, Q. Yu, B. Nadal, B. Bresson, M. Rosticher, N. Lequeux, A. Zimmers and H. Aubin, *Phys. Rev. Lett.*, 2011, **107**, 176803.
15 J.-F. Dayen, E. Devid, M. V. Kamalakar, D. Golubev, C. Guédon, V. Faramarzi, B. Doudin and S. J. van der Molen, *Adv. Mater.*, 2013, **25**, 400–404.
16 L. Clarke, M. N. Wybourne, L. O. Brown, J. E. Hutchison, M. Yan, S. X. Cai and J. F. W. Keana, *Semicond. Sci. Technol.*, 1998, **13**, A111.
17 S. Chen, *Anal. Chim. Acta*, 2003, **496**, 29–37.
18 R. Negishi, T. Hasegawa, H. Tanaka, K. Terabe, H. Ozawa, T. Ogawa and M. Aono, *Surf. Sci.*, 2007, **601**, 3907–3911.
19 N. Lidgi-Guigui, P. Seneor, F. Nguyen Van Dau, A. Friederich, A. Vaurès and C. Deranlot, *Appl. Phys. Lett.*, 2007, **90**, 233101.
20 H. Zheng, M. Asbahi, S. Mukherjee, C. J. Mathai, K. Gangopadhyay, J. K. W. Yang and S. Gangopadhyay, *Nanotechnology*, 2015, **26**, 355204.
21 M. Yun, B. Ramalingam and S. Gangopadhyay, *Nanotechnology*, 2011, **22**, 465201.
22 B. Ramalingam, H. Zheng and S. Gangopadhyay, *Appl. Phys. Lett.*, 2014, **104**, 143103.
23 S. E. Kubatkin, A. V. Danilov, A. L. Bogdanov, H. akan Olin and T. Claeson, *Appl. Phys. Lett.*, 1998, **73**, 3604–3606.
24 T. Ohgi and D. Fujita, *Surf. Sci.*, 2003, **532–535**, 294–299.
25 H. Graf, J. Vancea and H. Hoffmann, *Appl. Phys. Lett.*, 2002, **80**, 1264.
26 E. Speets, B. Dordi, B. Ravoo, N. Oncel, A.-S. Hallbäck, H. J. W. Zandvliet, B. Poelsema, G. Rijnders, D. H. A. Blank and D. Reinhoudt, *Small*, 2005, **1**, 395–398.
27 S. Gomez, L. Erades, K. Philippot, B. Chaudret, V. Collière, O. Balmes and J.-O. Bovin, *Chem. Commun.*, 2001, 1474–1475.
28 N. Decorde, N. M. Sangeetha, B. Viallet, G. Viau, J. Grisolia, A. Coati, A. Vlad, Y. Garreau and L. Ressier, *Nanoscale*, 2014, **6**, 15107–15116.
29 A. A. Middleton and N. S. Wingreen, *Phys. Rev. Lett.*, 1993, **71**, 3198.
30 K.-H. Müller, J. Herrmann, B. Raguse, G. Baxter and T. Reda, *Phys. Rev. B: Condens. Matter Mater. Phys.*, 2002, **66**, 075417.
31 T. B. Tran, I. S. Beloborodov, X. M. Lin, T. P. Bigioni, V. M. Vinokur and H. M. Jaeger, *Phys. Rev. Lett.*, 2005, **95**, 076806.
32 C. Duan, Y. Wang, J. Sun, C. Guan, S. Grunder, M. Mayor, L. Peng and J. Liao, *Nanoscale*, 2013, **5**, 10258.
33 M. Cargnello, A. C. Johnston-Peck, B. T. Diroll, E. Wong, B. Datta, D. Damodhar, V. V. T. Doan-Nguyen, A. A. Herzing, C. R. Kagan and C. B. Murray, *Nature*, 2015, **524**, 450–453.

34 C. T. Black, *Science*, 2000, **290**, 1131–1134.
35 C. E. McCold, Q. Fu, J. Y. Howe and J. Hihath, *Nanoscale*, 2015, **7**, 14937–14945.
36 A. L. Hickey and C. N. Rowley, *J. Phys. Chem. A*, 2014, **118**, 3678–3687.
37 J. Kane, M. Inan and R. F. Saraf, *ACS Nano*, 2010, **4**, 317–323.
38 J. Kane, J. Ong and R. F. Saraf, *J. Mater. Chem.*, 2011, **21**, 16846.
39 D. Greshnykh, A. Frömsdorf, H. Weller and C. Klinke, *Nano Lett.*, 2009, **9**, 473–478.
40 P. Yang, I. Arfaoui, T. Cren, N. Goubet and M.-P. Pileni, *Nano Lett.*, 2012, **12**, 2051–2055.
41 M. O. Blunt, M. Šuvakov, F. Pulizzi, C. P. Martin, E. Pauliac-Vaujour, A. Stannard, A. W. Rushforth, B. Tadić and P. Moriarty, *Nano Lett.*, 2007, **7**, 855–860.